

## Supporting Information

### Kinetic Stability of the Flavin Semiquinone in Photolyase and Cryptochrome-DASH

Michael J. Damiani, Gary N. Yalloway, Jessica Lu, Neahlanna R. McLeod, and Melanie A. O'Neill\*

Department of Chemistry, Simon Fraser University, Burnaby, B. C., Canada, V5A 1S6  
Correspondence: [maoneill@sfu.ca](mailto:maoneill@sfu.ca)

#### Contents

#### Page

S2	Figure S1	SDS-PAGE analysis of pure PL and PL mutants
S2	Figure S2	SDS-PAGE analysis of preparation of CRY-DASH
S3	Figure S3	Absorption spectra of fully oxidized proteins and released FAD cofactors
S4	Figure S4	Absorption spectra recorded during protein photoreduction
S5	Figure S5	Extinction spectra of photolyase in three redox states
S6	Figure S6	Control spectra: incubation of anaerobic reduced protein samples
S7	Figure S7	Absorption spectra of PL after long-term sq oxidation
S8	Figure S8	Comparative kinetic analysis for A385S-PL and W392Y-PL
S9	Figure S9	Evidence for proton-coupled electron transfer in CRY-DASH
S10	Figure S10	Spectroelectrochemical oxidative titrations of E1 in PL
S11	Figure S11	Comparison of spectroelectrochemical oxidative and reductive titrations with PL
S12	Figure S12	Comparison of spectroelectrochemical oxidative and reductive titrations with W392Y-PL
S13	Figure S13	Kinetics of disproportionation in wild-type PL and W392Y-PL
S14	Figure S14	Absorption spectra monitoring complete oxidation of Y398W-CRY-DASH
S15		Spectroelectrochemical Details

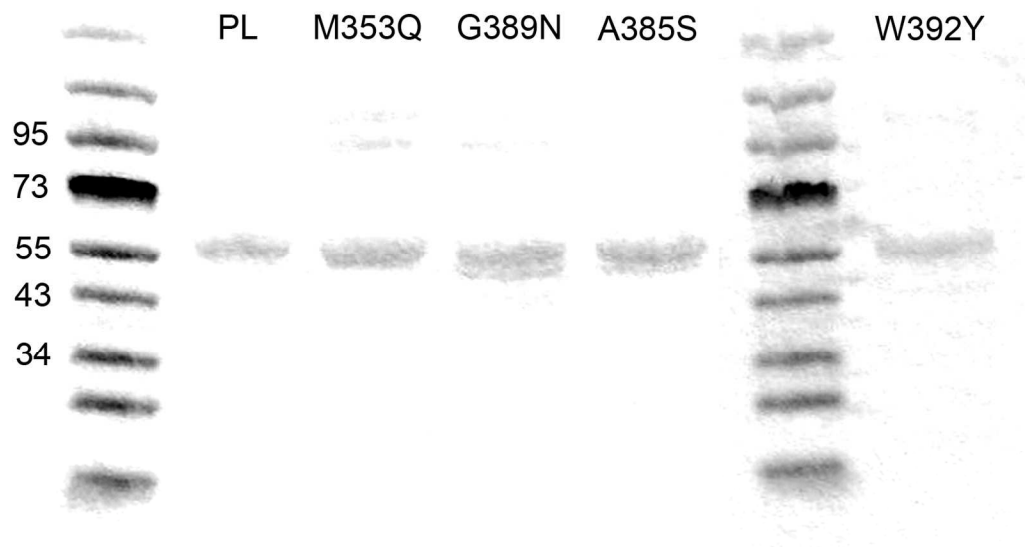


**Figure S1.** PL and PL mutants following complete purification (details in Materials and Methods). 7% SDS-PAGE gel stained with Coomassie Brilliant Blue shows each PL protein at the expected molecular weight (~55 kDa).

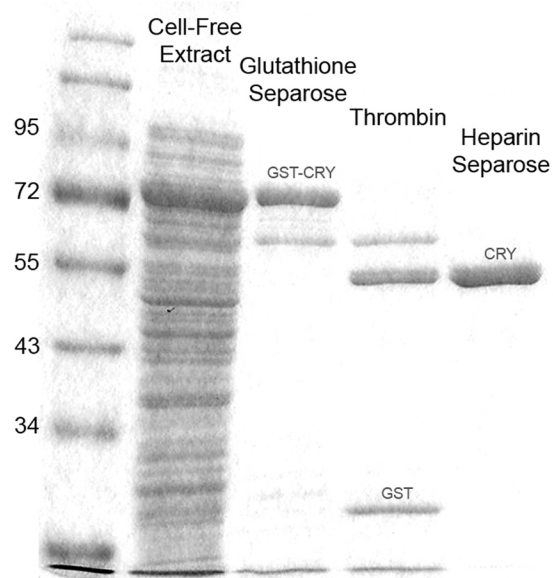


**Figure S2.** Purification of CRY-DASH. Representative 7% SDS-PAGE gel stained with Coomassie Brilliant Blue after each step of protein purification (details in Materials and Methods). CRY-DASH, overexpressed as a GST fusion protein (~82 kDa), is seen as a dark band in the cell-free extract lane. After eluting from the Glutathione-sepharose column, the protein is nearly pure with the exception of a co-eluting contaminant. This is removed following thrombin cleavage and purification on Heparin-sepharose.

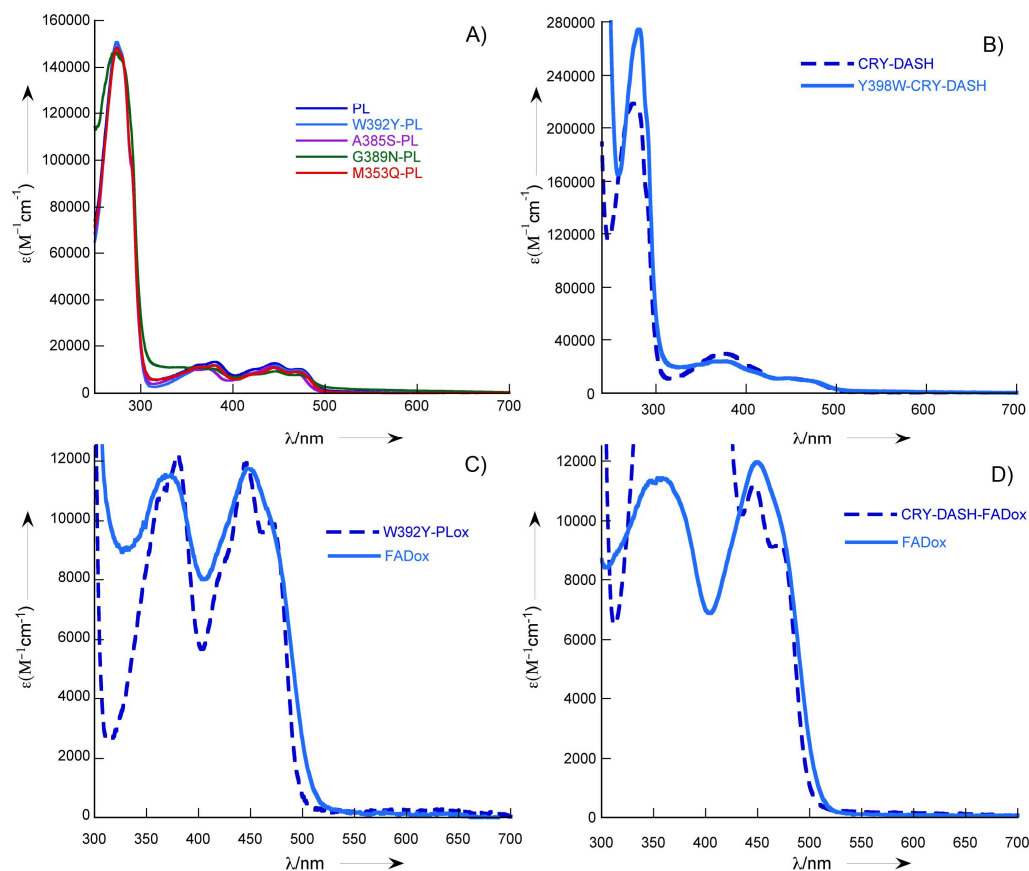


**Figure S3.** UV-Vis absorption spectra (plotted as extinction coefficient) of A) fully oxidized proteins PL, A385S-PL, M353Q-PL, G389N-PL and W392Y-PL showing ratio of absorptions at 280:440nm (normalized at 280 nm), indicative of the apoprotein:FAD stoichiometry  $\sim 1:1$  (details in Materials and Methods). B) Fully oxidized CRY-DASH and Y398W-CRY-DASH showing the ratio of absorptions at 280:380:440 nm, indicative of the apoprotein:MTHF:FAD stoichiometry. In wild-type CRY-DASH, the cofactor stoichiometry is typically  $\sim 1:0.8:0.7$ , while in Y398W-CRY-DASH it is  $\sim 1.0:0.6:0.5$ . C) W392Y-PL and D) CRY-DASH, fully oxidized after completion of  $\sim 48$  hour oxidation experiments and FAD cofactors released upon denaturation. The fine structure in the oxidized FAD absorption bands, seen only prior to denaturation, confirms that the FAD remains protein-bound throughout the oxidation experiments. The comparable absorbance before and after cofactor release indicates full oxidation in both cases. In CRY, the MTHF cofactor is responsible for the strong absorption between  $\sim 320$ -400 nm.

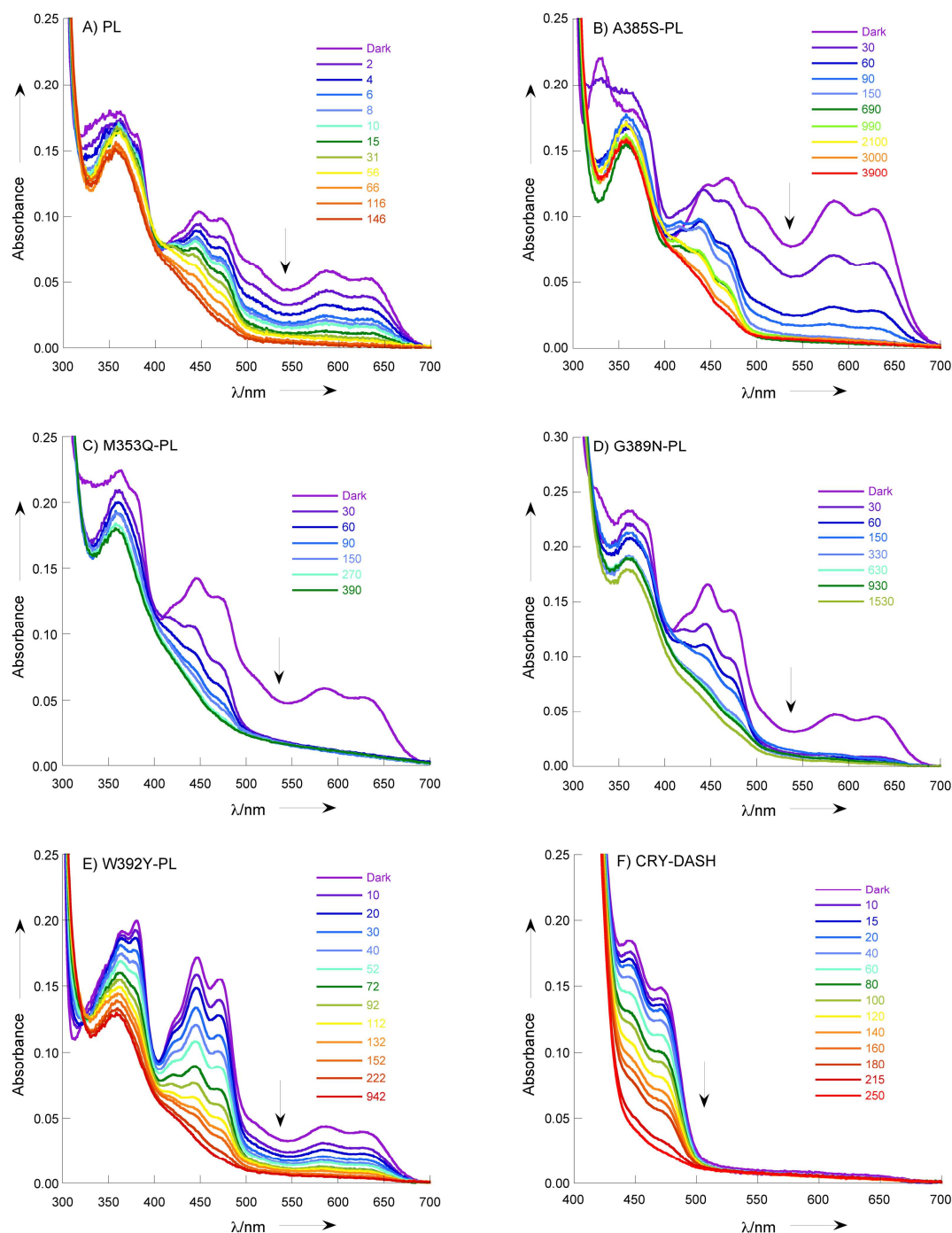


**Figure S4.** UV-Vis absorption spectra recorded during white light photoreduction of A) PL, B) A385S-PL, C) M353Q-PL, D) G389N-PL, E) W392Y-PL, and F) CRY-DASH in aqueous buffer containing 10 mM EDTA (pH 7). The concentration of holoproteins was 20-30  $\mu$ M. Numbers in the figures legend correspond to total irradiation time in seconds. Reduction was monitored by loss of absorbance at 580 nm (sq) and 450 nm (sq, ox). In the CRY spectra, the x-axis is truncated at 400 nm, below which absorption by the MTHF cofactor becomes dominant.

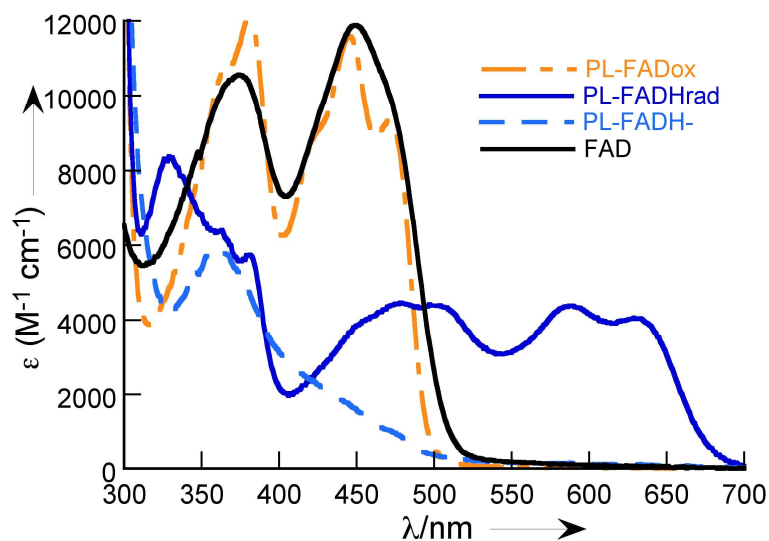


**Figure S5.** UV-Vis absorption spectra of the three redox states of FAD, bound to PL, in aqueous buffer (pH 7), and free oxidized FAD in the same buffer. The holoprotein concentration was  $\sim 20 \mu\text{M}$ . Extinction coefficient, plotted on the Y-axis, was determined from the absorption spectrum of the fully oxidized FAD released from each protein sample (with FADox  $\epsilon_{440} = 11300 \text{ M}^{-1} \text{ cm}^{-1}$ ). The hq spectrum was obtained by complete photoreduction of PL; the sq spectrum was obtained after near quantitative oxidation of the hq to the sq, where the concentration of sq accounts for the  $\sim 90\%$  of the FAD concentration; the ox spectrum was obtained after incubation for 3 days with 10 mM potassium ferricyanide followed by dialysis into storage buffer.

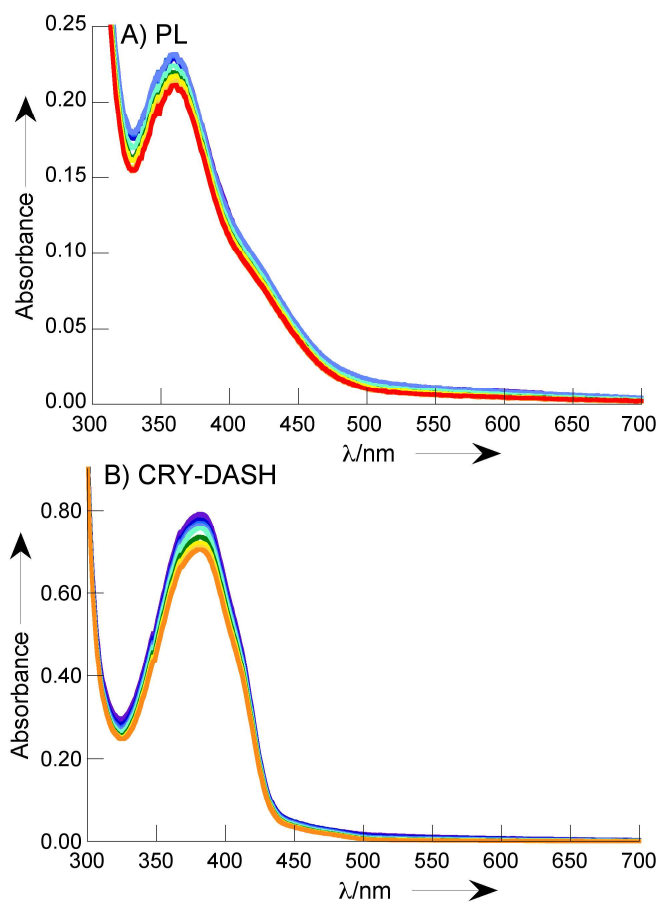


**Figure S6.** Time-dependence UV-Vis absorption spectra monitoring anaerobic samples of A) PL and B) CRY-DASH over a period of  $\sim 1500$ - $3000$  min. All conditions were matched to those in oxidation experiments, with the exception that  $O_2$  has been excluded. These control experiments establish that the spectral changes observed in oxidation experiments (e.g. Fig 3,4) require  $O_2$ . Note that large absorbance between  $\sim 320 - 400$  in the spectra of CRY corresponds to its MTHF cofactor.

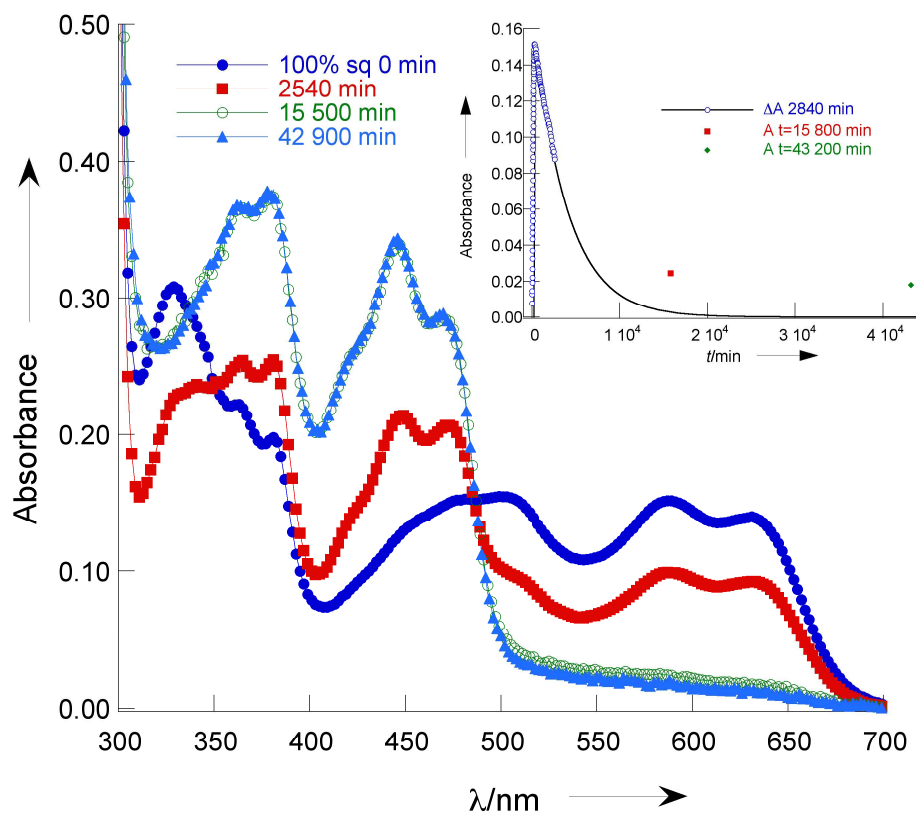


**Figure S7.** UV-Vis absorption spectra monitoring loss of sq in PL during extended exposure to  $O_2$ . Spectra were recorded  $\sim 2$  (2540 min),  $\sim 11$  (15500 min) and  $\sim 30$  (42900 min) days following quantitative generation of the sq by hq oxidation with  $O_2$ . Samples were stored at  $4^\circ C$  in the dark. Inset: The kinetics of oxidation monitored by absorption changes at 580 nm over a period of  $\sim 2800$  min, are fit to a first order growth and decay (line), which is extrapolated to complete sq decay. Data points (square + diamond) indicate measured absorbance from the spectra shown.

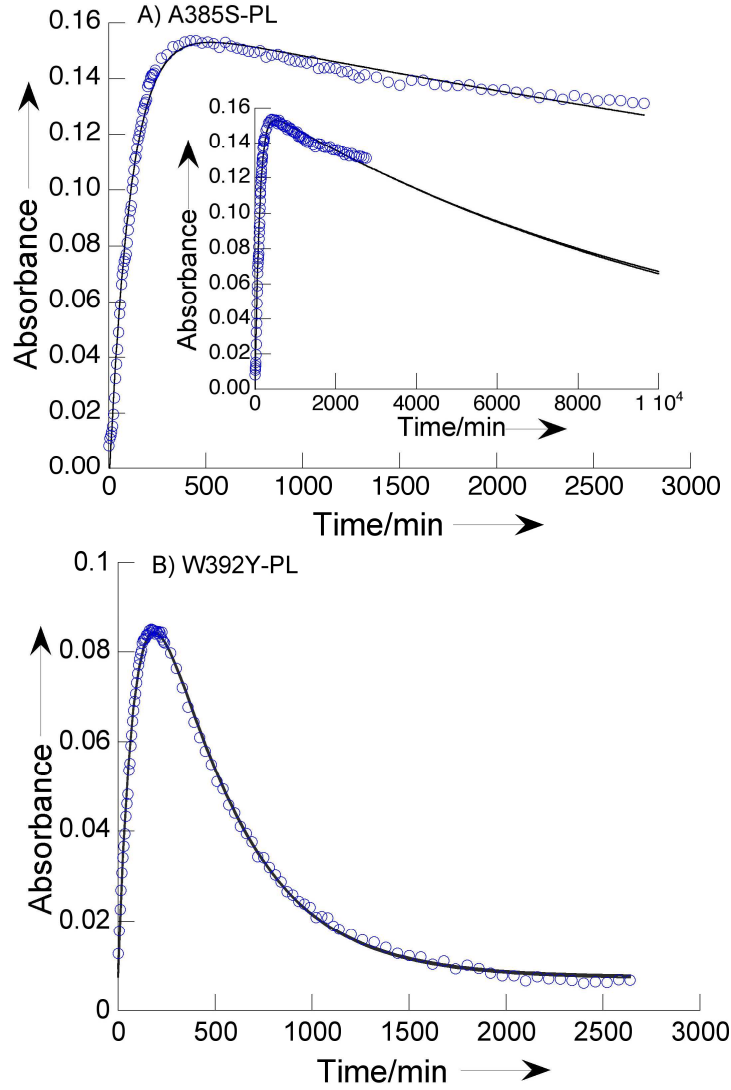


**Figure S8.** Time-dependent UV-vis absorption at 580 nm monitoring growth and decay of FAD sq in A) A385S-PL, and B) W392Y-PL, following introduction of O<sub>2</sub> to the fully reduced proteins. Lines represent fits of the experimental data (open circles) to an expression for the intermediate B, in an A to B to C kinetic scheme (eq. S1), or to an expression for a first order growth plus first order decay (eq. S2). In both expressions,  $A_{sq}^{\max}$  corresponds to the absorbance at 580 nm for 100% sq formation (*i.e.* equivalent to  $[hq]_o/\epsilon_{hq}$  in application of eq. 1-3). The two expressions produce identical fits to the data (lines superimposed), as expected when  $k_1 \gg k_2$ . The inset in A) shows the predicted profile of the models at long time, as compared to the experimental data measured over 2 days.

$$A_{sq} = A_{sq}^{\max} \frac{k_1}{k_2 - k_1} * (e^{-k_1 t} - e^{-k_2 t}) \quad (S1)$$

$$A_{sq} = A_{sq}^{\max} (-e^{-k_1 t} + e^{-k_2 t}) \quad (S2)$$



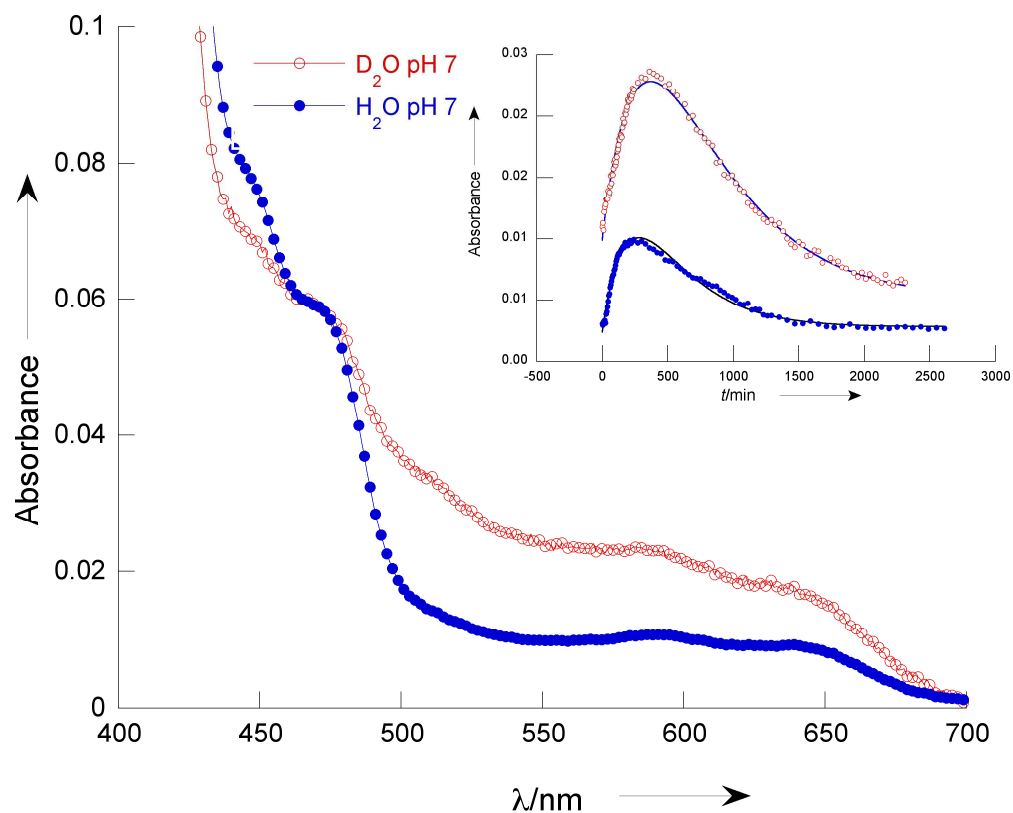


**Figure S9.** Kinetic isotope effect on oxidation of CRY-DASH sq. Spectra were taken at the time of maximum semiquinone accumulation following introduction of  $O_2$  to fully reduced CRY-DASH ( $\sim 25 \mu M$ ) exchanged into  $H_2O$  or  $D_2O$  buffer at pH 7. Inset: The kinetics of sq formation and oxidation monitored by absorption changes at 580 nm.

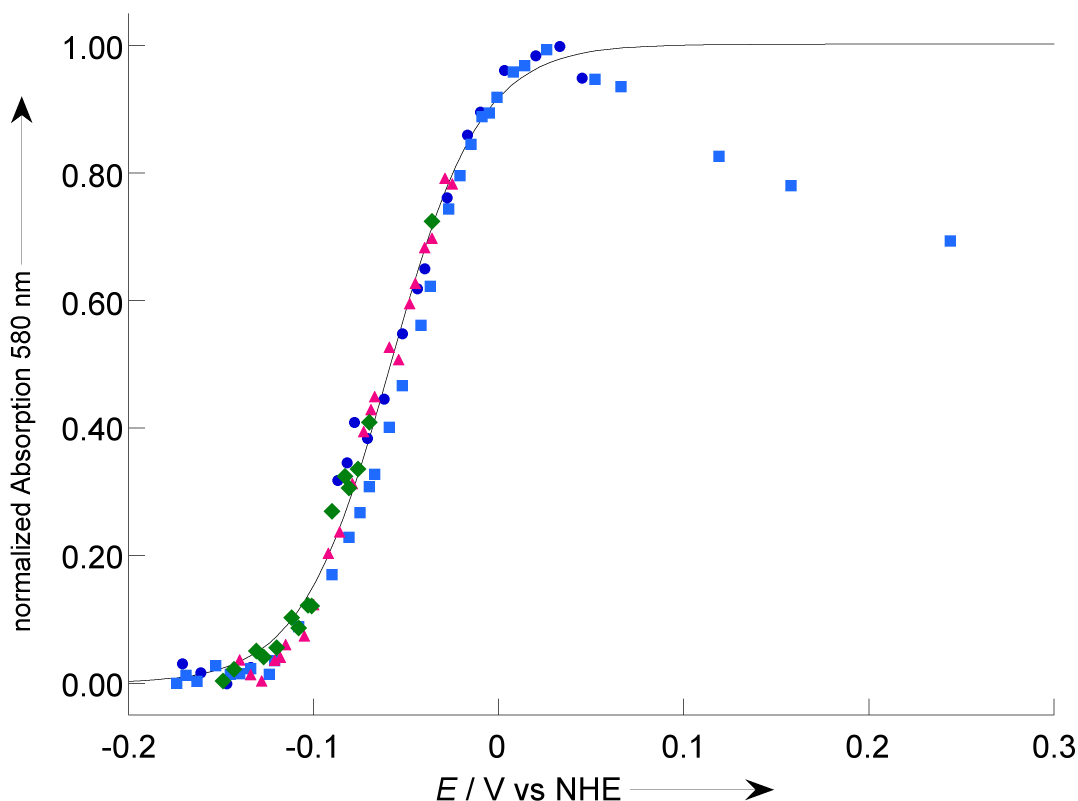


**Figure S10.** Spectroelectrochemical oxidative titration of PL in the presence of mediators (experimental details on S15).<sup>[1]</sup> Absorption of sq at 580 nm (4 trials), normalized for differences in protein concentration, is plotted versus potential; line is fit to a modified Nernst equation<sup>[2]</sup> yielding an  $E_1 = -58 \pm 6$  mV vs NHE (average and standard deviation from 4 trials). The protein was fully reduced to hq by the addition of degassed sodium dithionite and aliquots of potassium ferricyanide were added stepwise, oxidizing the protein from hq to sq (See Fig. S-11). After equilibration, the concentration of sq was determined by its absorption at 580 nm and the cell potential was recorded. After quantitative sq formation, equilibration times increased drastically. The points shown at positive potentials were recorded 3-5 hours after each addition of oxidant, and complete equilibration at each step may not have been achieved (these points were excluded from fit to the Nernst equation). However, partial oxidation of the sq is clearly evident by the loss of absorbance at 580 nm; concomitant formation of fully oxidized FAD was observed between 350-500 nm.

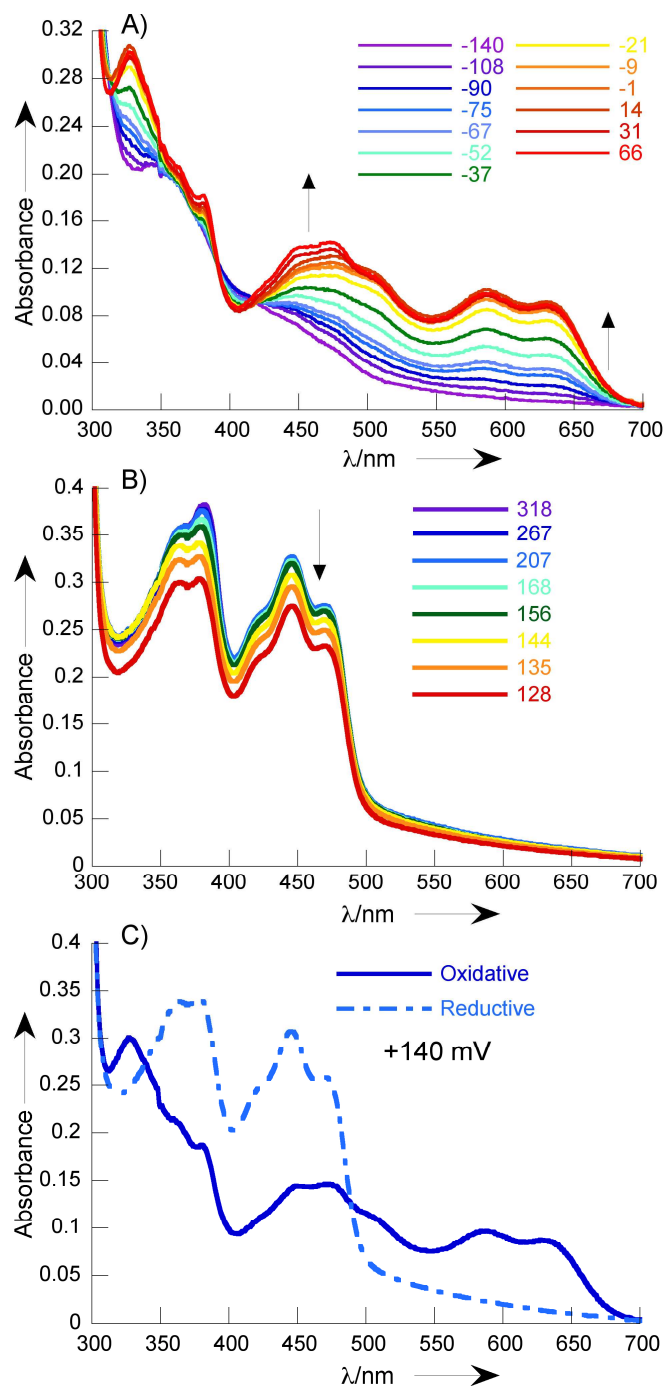


**Figure S11.** UV-vis absorption spectra taken during spectroelectrochemical A) oxidative and B) reductive titrations of PL in the presence of mediators (experimental details on S15). Legends display potential in mV vs NHE. C) Overlaid spectra from oxidative (purple solid line) and reductive (blue dashed line) titrations taken at the same measured potential of +140 mV vs NHE.

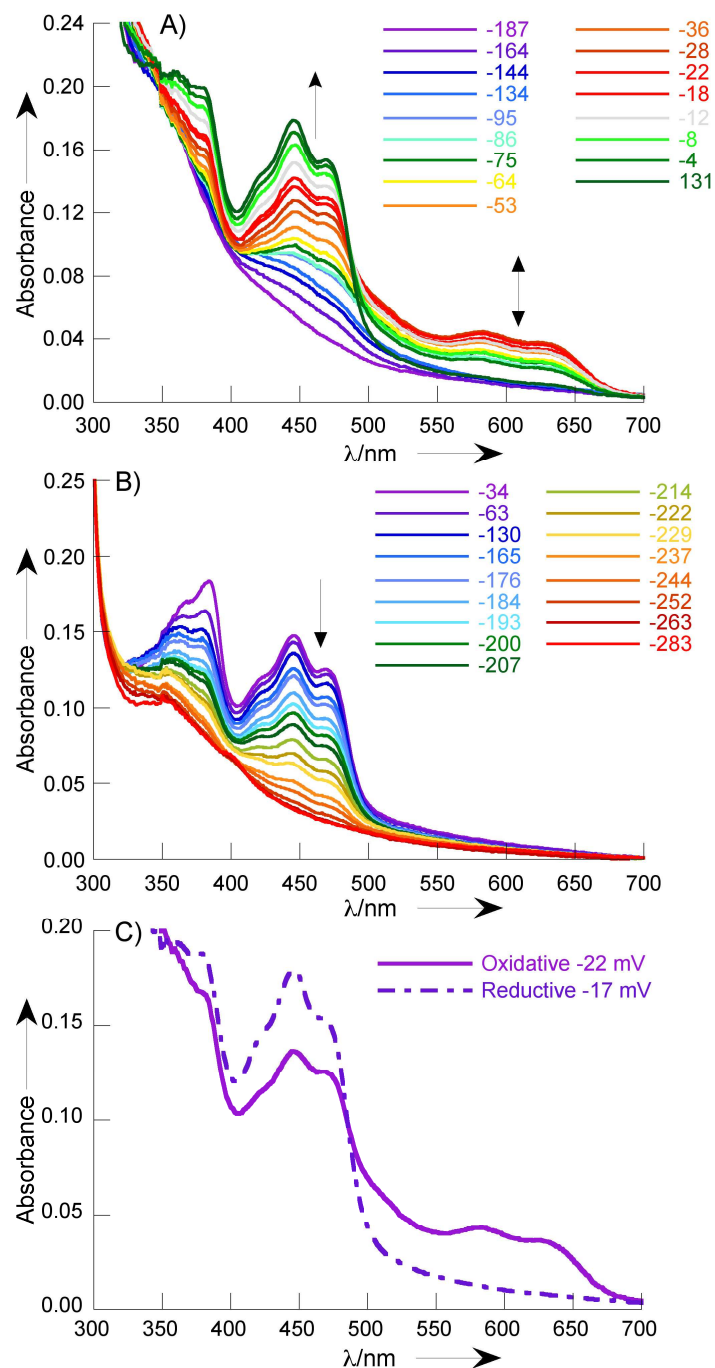


**Figure S12.** UV-vis absorption spectra taken during spectroelectrochemical A) oxidative and B) reductive titrations of W392Y-PL in the presence of mediators (experimental details on S15). Legends display potential in mV vs NHE. C) Overlaid spectra from oxidative (purple solid line) and reductive (blue dashed line) titrations taken at the similar measured potential of -22 and -17 mV vs NHE, respectively.

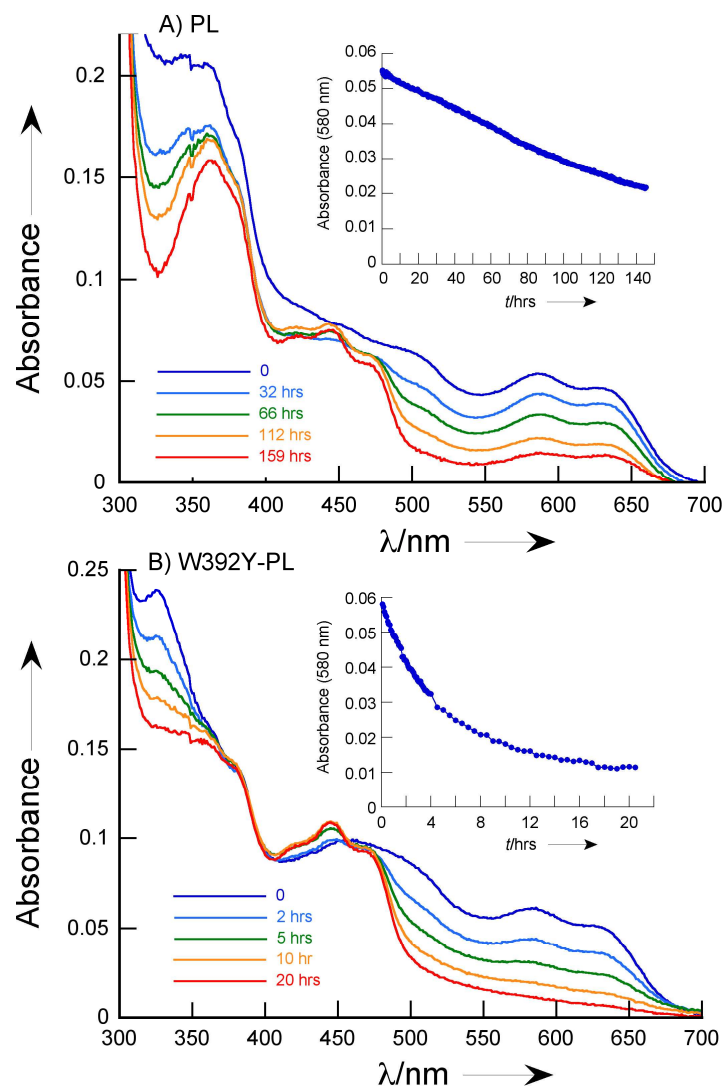


**Figure S13.** Time-dependent UV-vis absorption spectra following addition of 0.5 equivalents of potassium ferricyanide to anaerobic, fully reduced samples of A) PL and B) W392Y-PL. In both cases, the sq ( $\lambda \geq \sim 580$  nm) is observed to decay yielding bands characteristic of fully oxidized ( $\lambda \sim 420, 450$  nm), and fully reduced ( $\lambda \sim 360$  nm) FAD. The fine structure in the oxidized FAD absorption indicates that the cofactor remained bound throughout the experiment, and minimal precipitation is detected. No spectral corrections for this have been made. Insets: The distinct decay kinetics of the sq in wild type versus W392Y-PL.

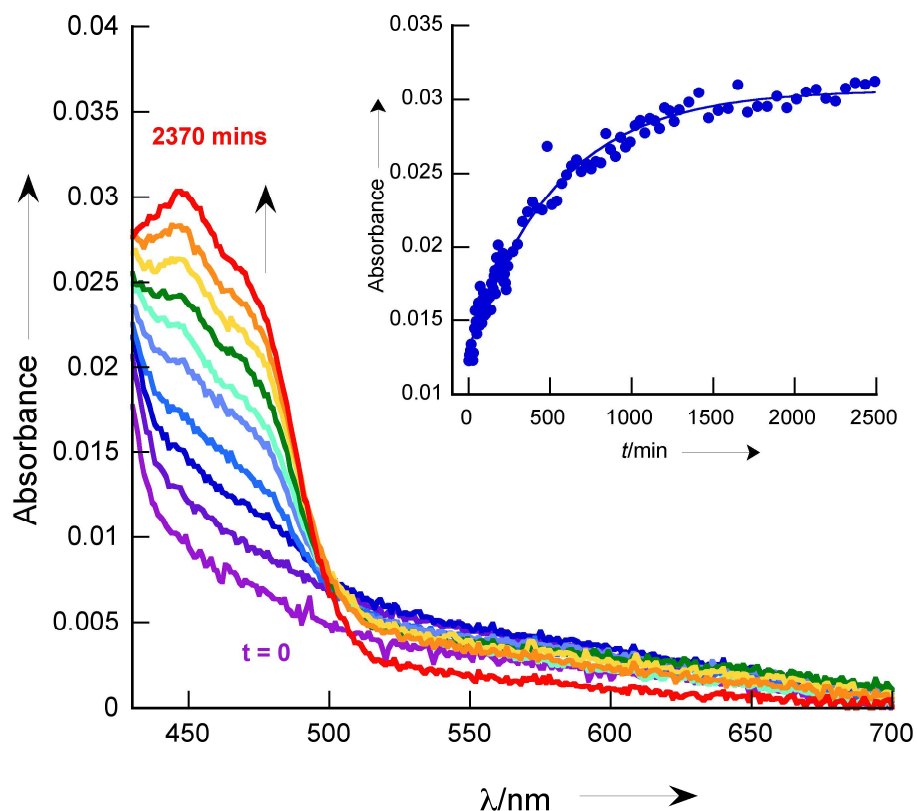


**Figure S14.** Time-dependent UV-vis absorption spectra monitoring complete oxidation of fully reduced Y398W-CRY-DASH. The protein concentration is  $\leq 10$ -fold lower than that used in analogous experiments with PL, W392Y-PL, and CRY-DASH. However, should the sq be stabilized as in PL, it would be clearly evident in these spectra; instead, little sq is detected. Inset shows the time-dependent absorbance at 445 nm due to ox formation. This kinetic profile is qualitatively similar to wild-type CRY-DASH. The region of the spectrum below 400 nm is dominated by absorption of the MTHF cofactor.

## Spectroelectrochemical Details

Protein samples (1.2 mL) in phosphate buffer (10 mM  $\text{KH}_2\text{PO}_4$ , 350 mM NaCl, 10% glycerol, pH 7) were contained in a quartz anaerobic cell (custom built) with a 1 cm path length and fitted with a platinum wire working electrode and a calomel reference electrode calibrated prior to the measurements (+257 mV at 10 °C, pH 7). Proteins were made anaerobic through 4 cycles consisting of evacuation/flushing with ultrapure argon; the cell was then sealed. The cell was equipped with an indicator side-arm filled with ~ 600  $\mu\text{L}$  of 3 mM methyl viologen, 3 mM EDTA and 40  $\mu\text{M}$  FAD in phosphate buffer. This oxidized mixture (transparent) was photoreduced (deep blue) with white light prior to each redox experiment. The indicator solution serves to soak up extraneous oxygen and provided a sensitive measure of its presence in the cell. Titrations were carried out in the following mediators: benzyl viologen (1  $\mu\text{M}$ ), 2-OH-1,4-naphthoquinone (15  $\mu\text{M}$ ), 2,5-dihydroxyl-1,4-benzoquinone (15  $\mu\text{M}$ ), 5,8-dihydroxyl-1,4-naphthoquinone (15  $\mu\text{M}$ ), duroquinone (15  $\mu\text{M}$ ), phenazine ethosulfate (1  $\mu\text{M}$ ), phenazine methylsulfate (1  $\mu\text{M}$ ), 1,2-naphthoquinone (15  $\mu\text{M}$ ) and anthroquinone-2-sulfonic acid (1  $\mu\text{M}$ ). The redox potential was adjusted stepwise (10-20 mV per step) by the addition of small volumes (~ 2.5  $\mu\text{L}$ ) of a concentrated solution (~ 1 mM) of either sodium dithionite as a reductant or potassium ferricyanide as an oxidant. Typical equilibration times were 20-45 minutes although equilibration times as long as 18 hrs. have been examined for some steps. Scan ranges varied between -300 to +300 mV vs NHE depending on the protein and experiment. After each step, the solution was allowed to equilibrate until the open circuit potential stabilized,  $\Delta E < 1\text{mV}/15\text{ mins}$ , and two or more identical UV-vis spectra are recorded. Absorption spectra recorded at each potential were corrected for scattering due to minimal precipitation by zeroing spectra at 715 nm. To extract the (hq/sq) potential  $E_1$ , changes in absorption of the sq (580 nm) with potential (Fig. S10) are fit to a modified Nernst equation where  $A$  is the total absorbance,  $a$  is the absorbance value contributed by the sq,  $E_1$  is the hq/sq potential and  $E$  is the measured potential.

$$A_{580} = \epsilon_{580}a / 1 + \exp\left[\frac{nF}{RT}(E_1 - E)\right]$$

## REFERENCE

1. P. L. Dutton, *Methods Enzymol.* **1978**, *54*, 411-435.